




Unveiled materials and techniques in wall paintings hidden for centuries in the church of San Francesco del Prato (Parma, Italy)

Laura Fornasini^{1,a} , Simona Raneri², Stefano Legnaioli², Vincenzo Palleschi², Antonella Casoli³, Silvia Simeti⁴, Danilo Bersani¹

¹ Department of Mathematical, Physical and Computer Sciences, University of Parma, Parco Area delle Scienze 7/A, 43124 Parma, Italy

² ICCOM-CNR, Institute of Chemistry of Organometallic Compounds, National Research Council, Via G. Moruzzi 1, 56124 Pisa, Italy

³ Department of Chemistry, Life Sciences and Environmental Sustainability, University of Parma, Parco Area delle Scienze 17/A, 43124 Parma, Italy

⁴ Arché Restauri snc di Simeti Silvia & C, Via Chiavari 18/A, 43125 Parma, Italy

Received: 28 October 2022 / Accepted: 12 January 2023

© The Author(s) 2023

Abstract The church of San Francesco del Prato in Parma (Italy) is a masterpiece of the Gothic style, dated back to the 13th century. However, its historical and monumental value could not be appreciated for a long time, especially due to the transformation of the building into a city jail. The recent restoration works brought back to light valuable frescos and wall paintings belonging to different periods. An in situ campaign was performed on the 15th-century wall paintings adorning the vault and the walls in the church apse, by using mobile Raman and X-ray fluorescence equipment. The characterization of the art pieces was further carried out with micro-Raman spectroscopy and gas chromatography–mass spectrometry analyses. Overall, a quick and thorough identification of the colours palette of the wall paintings was successfully obtained through the in situ measurements. Laboratory analyses corroborated the understanding of the techniques through the identification of pigments and binders. In addition, micro-Raman analyses highlighted the presence of degradation products. Interestingly, a pigment hierarchy has been noted in relation to the painted contents, enhancing the preciousness of holy figures and their distinctive details.

1 Introduction

According to Pelicelli's hypothesis [1, 2]—spread over time but not always shared [3], due to the almost total absence of recent monographic studies and the dispersion of a large part of the Fabbrica Archive—the church of San Francesco del Prato in Parma (Italy) was built in three construction campaigns starting from a single initial project, consisting of a triapsidal basilica plan with a trussed roof (ante 1298, ante 1398, 1443); only the apses covered by vaults, in accordance with the prescriptions for the construction of Franciscan churches in the *Statuta capituli generalis Narbonensis* by Bonaventura da Bagnoregio (1260). The church was built *extra moenia* on a portion of the Prato Regio, a place designated for religious fairs, military contests and trade since the Lombards era, thanks also to its strategic position with respect to the water communication routes with the outside world. In 1804, the Napoleonic suppression of the church and the adjoining convent led to a profound transformation of the building, which was then used as a jail until 1992 [4]. Successively, the property was first transferred to the Franciscan Order and then to the University of Parma until 2017, when the church was handed back to the Agenzia del Demanio (State Property Agency), followed by its concession of use to the Diocese.

Starting in 2018, a complex architectural and structural restoration was carried out to recover the building. In conjunction with this intervention, partial conservative restorations were realized on the damaged decorated surfaces, hidden by thick layers of spurious plasters and “scialbi” (thick layers of slaked lime applied on wall paintings in order to cover them. Usually, the covering of a wall paintings can be related to a change in the aesthetic taste of a certain period, hygienic reasons or a poor state of conservation.) and altered by the architectural distortion during the detrimental transformation into a jail, that largely destroyed that 15th-century wall paintings in the church (side aisles, columns, etc.).

The recovery of the wall paintings in the central apse—vaults and walls—started from a meticulous and complex “descialbo” intervention (the controlled removal of the “scialbo” from wall paintings) on all the surfaces: wall paintings were not visible except for a few sections, which were furthermore distorted by previous improper restorations.

Tampering, degradation and neglect of the church for centuries have clearly affected the survival of the complex fresco decoration of the apse, finished with precious *a secco* details, dating back to the 15th century. The severely damaged and missing decoration

Focus Point on Scientific Research in Cultural Heritage 2022 Guest editors: L. Bellot-Gurlet, D. Bersani, A.-S. Le Hô, D. Neff, L. Robinet, A. Tournié.

^a e-mail: laura.fornasini@unipr.it (corresponding author)

of the vault originally showed a blue sky with stars and golden “studs” and a refined lace frame framing the ten rib vaults which are separated by painted veining with geometric motifs that branch out from the keystone. Inside, a carved and painted polychrome stone *tondo* depicts the subject of Christ Blessing, with extremely refined plastic details and its polychrome clothing. On the large rib vault, the subject of God Father was realized in a *mandorla* frame with a *pelta* motifs and angels, at the sides the figures of “Justice” and probably of “Faith”, almost completely lost. The upper part of the walls was adorned with figures of saints related to the Franciscan Order, which sometimes reported their names painted with Gothic characters. Unfortunately, large sections have been destroyed by the aperture of spurious windows—later walled up—above the original ogival windows. The decoration was enriched with sinuous and rich floral motifs with monochrome clypeus of different male busts portrayed with an accurate physiognomic characterization; starting capitals of the rib vaults that make a change of register with red veining descending to the floor; walls with monochrome ivory-white plaster echoing the colours of the central nave of the church. There are also further decorations on the walls, superimposed on the original plaster, such as the large frame of typical late 17th-century style painted on both the north and the south sides; in addition, under the latter, two precious and admirable frescoes dating back to the sixteenth century have emerged, which were completely unknown from the documents.

Despite the forced interruption of the restoration works—started in April 2020 then blocked in February 2021—an important unpublished page of the 15th and 16th-century artistic production in Parma is being offered to the community of art historians to be further studied and investigated in order to determine the authorship and the scope of production. The names of Bartolino de’ Grossi and Iacopo Loschi, traditionally supposed to be the authors of the frescoes in the apse (~ 1462), will have to be confirmed or not by the study of the surviving frescoes now visible. Detailed studies may also reveal the identity of the artists who realized the 16th-century frescoes, whether our suggestion—based on the artists’ style prior to more in-depth studies, clearly required—pointing at the sphere of G. Bedoli and M. Anselmi will be validated. These artists were active around the ‘30 s of the sixteenth century, together with F. M. Rondani, for the decoration of the so-called Oratorio della Concezione, a large chapel detached from the church during the jail period and now rejoined to it.

In this work, an in situ campaign was performed on the valuable 15th-century wall paintings adorning the vault and the walls in the church apse, by using mobile Raman and X-ray fluorescence equipment. The campaign was carried out in 2020, during the restoration works. Pigments and binders of the art pieces were further investigated with laboratory micro-Raman spectroscopy and gas chromatography–mass spectrometry analyses, by collecting representative submillimetre-sized fragments during the in situ campaign. Essential results on the colours palette and binders used by the artists were obtained. Degradation products were also detected as an effect of atmospheric pollutants on carbonaceous materials. The in situ measurements with mobile equipment proved to be effective in a quick and thorough identification of the pigments of the wall paintings. Laboratory analyses corroborated the understanding of the techniques and the degradation products.

2 Materials and methods

The in situ campaign was performed on the 15th-century wall paintings of the vault and the walls of the church apse through mobile Raman and X-ray fluorescence (XRF) equipment. In situ Raman analyses were realized through a mobile instrument i-Raman[®] Plus (BWTEK, USA) which presents a diode laser source emitting at 785 nm. Spectra were acquired between 60 and 3300 cm^{-1} with a spectral resolution of $\sim 3.5 \text{ cm}^{-1}$ @ 614 nm, with an exposure time of 10 s per acquisition and a laser power below 2.5 mW. In situ XRF measurements were carried out using the Elio portable XRF Analyzer (Bruker), equipped with a 10–40 keV/5–200 μA X-ray tube (Rh anode, 1 mm collimated beam on the sample) and a large area Energy Dispersive Si-Drift detector (130 eV FWHM at Mn K).

During the in situ campaign, twenty-five representative submillimetre-sized fragments were collected by means of a scalpel and laboratory analyses were performed through micro-Raman spectroscopy and gas chromatography–mass spectrometry.

Micro-Raman measurements were collected with two micro-spectrometers: a Horiba Jobin Yvon LabRam confocal micro-spectrometer (300 mm focal length) equipped with a He–Ne 632.8 nm, an integrated Olympus BX40 microscope with 4 \times , 10 \times , 50 \times ULWD and 100 \times objectives, a 1800 lines/mm grating, a XY motorized stage and a Peltier cooled Si CCD. Additional micro-Raman measurements were performed with a Horiba Jobin Yvon LabRam HR Evolution confocal micro-spectrometer (800 mm focal length) by using a He–Ne 632.8 nm, an integrated Olympus BX40 microscope with 5 \times , 10 \times , 50 \times ULWD and 100 \times objectives, a 600 lines/mm grating, a XY motorized stage and a liquid nitrogen cooled CCD. The spectral resolution was $\sim 2 \text{ cm}^{-1}$. The systems were calibrated with the 520.6 cm^{-1} Raman peak of silicon and the emission lines of a gas lamp. Data analysis was performed with the *LabSpec 5* built-in software. The fluorescence background was removed by a polynomial curve subtraction.

Gas Chromatography–Mass Spectrometry (GC–MS) analyses were performed by using a Trace 1300 Gas Chromatograph (Thermo Scientific) coupled to Agilent Technologies ISQ mass spectrometer, with single quadrupole and split-splitless injector. Samples were injected in splitless mode at 280 °C. The separation of the components was done by means of a SLB[®]-5 ms Capillary GC Column (L \times I.D. 30 m \times 0.25 mm, d_f 0.25 μm) by Sigma-Aldrich Supelco. The carrier gas (He, purity 99.995%) was used in constant flow mode at 20 mL/min. The mass spectrometer was operated in the EI positive mode (70 eV). Samples (about 1 mg) taken from the wall paintings were subjected to hydrolysis and derivatization treatment, according to a method previously studied and applied for the GC–MS analyses of fatty acids and amino acids contained in organic binders [5, 6].



Fig. 1 Selection of pictures of the analysed areas of the 15th-century wall paintings of the vault and walls of the church apse

3 Results and discussion

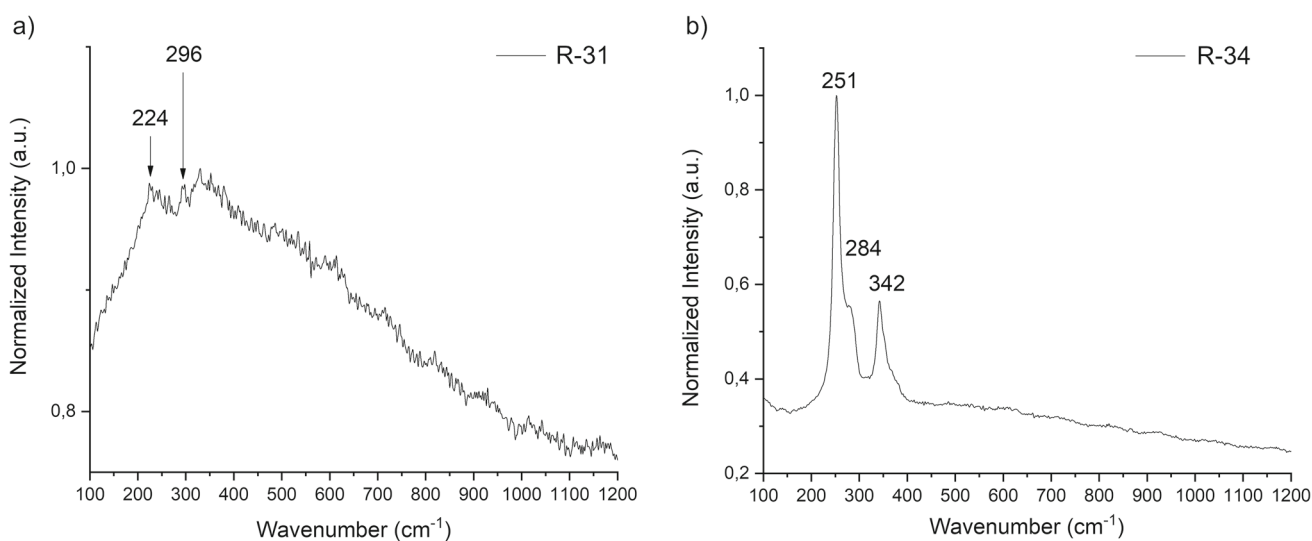
The 15th-century wall paintings adorning the vault and the walls of the church apse were investigated by in situ measurements with Raman and XRF equipment; micro-Raman spectroscopy and GC–MS analyses were also carried out on submillimetric samples collected during the in situ campaign. A selection of the investigated areas is reported in Fig. 1. Detailed pictures with all the analysed points are reported in the Supplementary Information (SI) (Figs. S1–S4). Through the Raman and the XRF measurements, the colours palette was characterized by analysing figures and details with different colours (black, blue, brown, golden, grey, green, pink, red, white and yellow), to identify the pigments. In addition, degradation products were also recognized. The binders were identified by GC–MS analysed. In the following sections, the results obtained with the multi-analytical approach will be reported and discussed.

3.1 In situ Raman and XRF measurements

The overall results obtained from the in situ Raman measurements are summarized in Table 1. In some cases for different samples, the peak positions referred to the same pigment are slightly different (see Table 1). A small shift in the peak positions is expected in some pigments (e.g., hematite or carbon black) for a slight local heating of the point of analysis during the collection of the spectrum. In addition, small shifts may be produced by minor differences in the chemical composition of a pigment, without involving a different compound. The obtained results are in agreement with the spectra from the literature and the identification of the pigments was possible [7–9].

Table 1 Pigments identified with mobile Raman spectroscopy on the 15th-century paintings

Sample	Colour	Analysed detail	Raman peaks (cm^{-1})	Attribution
R-30	Yellow	Pope's crown (wall #8)	135, 331	Lead tin yellow II
R-31	Red	Background (large rib vault)	224, 296	Hematite
R-32	Red	God's mantle (large rib vault)	251, 344 / 224, 290	Vermilion / Hematite
R-34	Red	Jesus's book (keystone)	251, 284, 342	Vermilion
R-36	Red	Jesus's cross (keystone)	251, 284, 342	Vermilion
R-38	Red	Jesus's lips (keystone)	251, 284, 342	Vermilion
R-40	Black	Architectural detail (wall #9)	1345, 1592	Carbon black
R-42	Black	Background (wall #8)	1342, 1595	Carbon black
R-43	Black	Frame (rib vault)	1346, 1590	Carbon black
R-45a	Red	Pope (wall #8)	251, 284, 342	Vermilion
R-45b	White	Pope (wall #8)	1085	Calcite

**Fig. 2** **a** Hematite Raman spectrum from the sample R-31, acquired with a 785 nm instrument and an integration time of 20 s. The background signal has not been reduced; however, the main peaks at 224 and 296 cm^{-1} are detectable. **b** Vermilion Raman spectrum from the sample R-34 acquired with a 785 nm instrument and an integration time of 20 s, showing the main peaks at 251, 284 and 342 cm^{-1}

Detailed pictures showing the analysed points are reported in the SI (Fig. S1). It is interesting to note that the red tones were obtained by selectively using different pigments, according to the depicted content. The Raman spectra revealed the use of hematite ($\alpha\text{-Fe}_2\text{O}_3$) in the background in the large rib vault [7]. Differently, the use of vermilion (HgS) was preferred to represent details of the holy subjects, like the book, the lips and the cross of Jesus in the keystone [8]. In the mantle of God, both vermilion and hematite were detected. Representative spectra obtained on red tones are shown in Fig. 2. Pope's crown was obtained with lead tin yellow II ($\text{PbSn}_{1-x}\text{Si}_x\text{O}_3$) [8]. White parts showed the presence of calcite (CaCO_3). On black details, the Raman spectrum of amorphous carbon suggested the use of carbon black.

The overall results obtained from the in situ XRF measurements are shown in Table 2. Detailed pictures showing the analysed points are reported in the SI (Fig. S2). The elemental composition of the red tones confirmed the Raman results. The detection of vermilion was supported by the presence of Hg and S in the XRF spectrum, which were found in the book and in the hand of Jesus (Fig. 3).

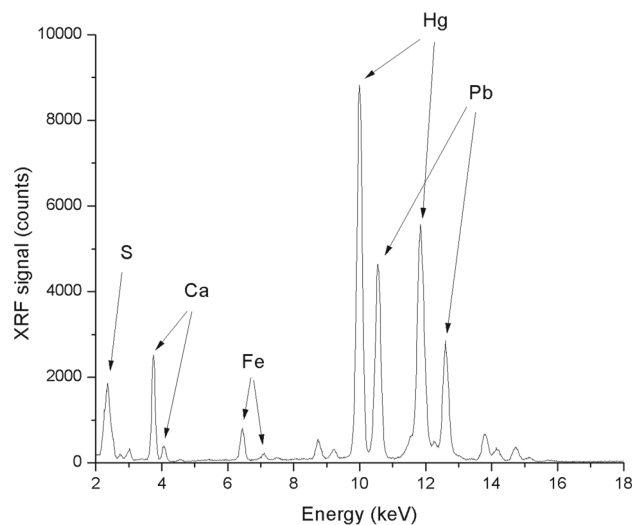
Other red and pink tones showed the signal of Fe, confirming the presence of iron oxides as pigments (red ochre, hematite). The use of ochres consisting of iron oxides/oxyhydroxides is also found in brown and yellow/golden details, except for the mantle of Jesus, whose chemical composition suggested the presence of lead–tin yellow. In blue and blue-black areas, high amount of Cu is compatible with Cu-based pigments, such as azurite. Similarly, Cu-based pigments were detected in green depicted contents.

3.2 Laboratory micro-Raman spectroscopy and GC–MS analyses

Twenty-five representative samples were collected during the in situ campaign by removing submillimetre-sized fragments from the paintings. Detailed pictures showing the sampling areas are reported in the SI (Figs. S3–S4).

Table 2 Main elements identified with XRF on the 15th-century paintings

Sample	Colour	Main elements
X-1	Red	Ca, Fe, Sr, Mn, Ba, S, Si, K
X-2	Pink	Ca, Fe, Sr, Mn, Ba, S, Si, K
X-3	Black	Fe, Sr, Pb, Cu, Zn, Mn, Ca, Ba, S, K, Si
X-4	Blue–black	Fe, Sr, Pb, Cu, Zn, Mn, Ca, Ba, S, K, Si
X-5	Brown	Fe, Mn, S, Ca, Sr, Si, Pb (scarce), Cu (scarce), Zn (scarce)
X-6	Brown	Fe, Mn, S, Ca, Sr, Si, Pb (scarce), Cu (scarce)
X-7	Brown	Fe, Mn, S, Ca, Sr, Si, Pb (scarce), Cu (scarce)
X-8	Golden	Pb (scarce), Sr, Mn, Fe, Ca, Ba, S
X-9	Blue–black	Fe, Sr, Cu, Zn, Mn, Ca, Ba, S, K, Si
X-10	Golden	Pb (scarce), Sr, Mn, Fe, Ca, Cu (scarce), Ba, S
X-11	Blue-Black	Fe, Sr, Cu, Zn, Mn, Ca, Ba, S, K, Si
X-12	Green	Pb, Cu, Fe, Ca, Ba, S
X-13	Green	Pb, S, Ca, Sr, Fe, Cu (scarce), Sn, Hg (scarce)
X-14	Red–yellow	Pb, S, Ca, Sr, Fe, Cu (scarce), Sn, Mn (scarce)
X-15	Red	Pb, S, Hg, Ca, Ba, Sr, Fe
X-16	Golden	Pb (scarce), Cu, Sr, Mn, Fe, Ca, Ba, S, P
X-17	Flesh pink	S, Ca, Pb, Hg, Sr
X-18	Green	S, Ca, Cu, Fe, Mn, Pb, Sr, Si, K
X-19	Dark green	S, Ca, Cu, Fe, Mn, Pb, Sr, Si, K
X-20	Green	S, Ca, Cu, Fe, Mn, Pb, Sr, Si, K
X-21	Green	S, Ca, Cu, Fe, Mn, Pb, Sr, Si, K
X-22	Green	S, Ca, Cu, Fe, Mn, Pb, Sr, Si, K
X-23	Green	S, Ca, Cu, Fe, Mn, Pb, Sr, Si, K
X-24	Blue	S, Ca, Fe, Mn, Pb, Sr, Si, K
X-25	Blue	S, Ca, Cu, Fe, Mn, Pb, Sr, Si, K
X-26	Blue	S, Ca, Cu, Fe, Mn, Pb, Sr, Si, K
X-27	Blue	S, Ca, Cu, Fe, Mn, Pb, Sr, Si, K

Fig. 3 XRF spectrum of the red spot X-15. The intense lines of Hg and S indicate the presence of Vermilion

Micro-Raman analyses supported and corroborated the recognition of pigments. The proper identification was confirmed by the comparison with data from the literature [7–13]. The overall identification obtained from the micro-Raman measurements are shown in Table 3. The results obtained with the mobile equipment were confirmed by the micro-Raman spectra. In the red part of a lateral decoration on a rib vault (LR-15), hematite was detected by the peculiar signals at 228, 247, 294, 413, 500, 614 and ~670 cm^{-1} , along with calcite (1086 cm^{-1}) (Fig. 4) [7, 8]. The mantle of Pope (LR-29) was realized with both hematite and vermilion, showing its contributions at 252 and 342 cm^{-1} (Fig. 4) [8]. A pigment hierarchy emerged in the realization of different details: holy figures (Jesus, Pope) and their distinctive features were typically obtained by using vermilion, a more expensive pigment compared to

Table 3 Pigments identified by means of micro-Raman spectroscopy on the 15th-century paintings

Sample	Colour	Analysed detail	Attribution
LR-15	Red	Lateral decoration (rib vault #3)	Hematite/Calcite
LR-16	Green	“Faith” figure (large rib vault)	Malachite/Gypsum/Calcite
LR-17	Black	Geometric motif (rib vault #3)	Carbon black/Gypsum
LR-18	Yellow	Geometric motif (rib vault #5)	Goethite
LR-19	White	Lateral decoration (rib vault #6)	Calcite/Gypsum
LR-20	Blue	Sky (rib vault #7)	Azurite/Calcite
LR-21	Brown–white	Veining (rib vault #7)	Hematite/Gypsum/Carbon black
LR-22	Pink–green	Flesh of hand’s angel (large rib vault)	Hematite/Calcite/Gypsum/Green earth
LR-23	Yellow	<i>A pelta</i> frame (large rib vault)	Goethite/Gypsum/Hematite/Calcite
LR-24	Light grey	Architectural detail (wall #9)	Calcite/Gypsum/Carbon black
LR-25	Dark grey	Architectural detail (wall #9)	Calcite/Gypsum/Carbon black
LR-26	Yellow	Architectural detail (wall #8)	Hematite/Calcite/Gypsum
LR-28	Green	Background (wall #9)	Malachite/Calcite
LR-29	Red	Pope’s mantle (wall #8)	Vermilion/Hematite
LR-30	Pink	Architectural detail (wall #6)	Hematite/Calcite/Gypsum
LR-31	Green	Veining (wall #1–2)	Malachite/Weddellite
LR-32	Yellow	Racemes of flowers (wall #8)	Litharge/Calcite
LR-33	Blue	Racemes in clypeus (wall #7)	Azurite/Barite/Weddellite
LR-36	Blue	Sky (keystone)	Azurite/Calcite/Gypsum

hematite, which was preferred for the decoration of large background areas. Yellow tones showed the use of further pigments, like goethite (α -FeOOH) with peaks at 300 and 390 cm^{-1} [7], which was identified in a *pelta* frame of the large rib vault (LR-23), and litharge (α -PbO) with peaks at 138 and 325 cm^{-1} [12] in the decoration of racemes of flowers on a wall (LR-32) (Fig. 5). On the white parts of white or light grey samples (LR-19, LR-24), calcite (155, 282, 712, 1086 cm^{-1}) and gypsum (414, 1008, 1133 cm^{-1}) in a lower amount were found (Fig. 6) [8]. Black and dark gray tones (LR-17, LR-24, LR-25) included carbon black, detected by the broad bands of amorphous carbon at ~ 1360 and ~ 1600 cm^{-1} (Fig. 6). Typically, also traces of calcite and gypsum were detected on dark details (Fig. 6). The observation of low amount of gypsum related to the presence of calcite suggested its formation as a degradation product due to the sulfatation process of calcium carbonate [14]. Azurite ($\text{Cu}_3(\text{CO}_3)_2(\text{OH})_2$) and malachite ($\text{Cu}_2(\text{CO}_3)(\text{OH})_2$) were used in some *a secco* green and blue areas: the sky in the keystone of the vault (LR-20), the figure personifying “Faith” in the large rib vault (LR-16) and in the decoration with racemes of flowers in a wall (LR-31) and in the sinuous motif in a clypeus (LR-33) (Fig. 7). In blue decorations (LR-33) and in the sky (LR-20 and LR-36), the signals of azurite were detected at 248, 400, 765, 835 and 1095 cm^{-1} [13]. In one case (in LR-33), the signal of barite (BaSO_4) was detected along with the azurite pigment (sharp peak at 988 cm^{-1}). Malachite was observed in details of the figure personifying “Faith” (LR-16), in green decoration (LR-31) and background (LR-28), with characteristic signals at 181, 269, 432, 507, 534, 1060, 1090 cm^{-1} [13]. Interestingly, in a green background corresponding to the end of a section (*giornata*), malachite was found (LR-28). In some whitish crystals in the fragments containing azurite or malachite, signals at 190, ~ 500 and ~ 905 cm^{-1} were observed, suggesting the presence of calcium oxalate dihydrate (weddellite, $\text{CaC}_2\text{O}_4 \cdot 2\text{H}_2\text{O}$). The observation of calcium oxalates (weddellite and/or whewellite) has been widely investigated in wall paintings: their formation may be ascribed to a biological activity (lichens, fungi, algae) or to a chemical degradation of an organic compound used as a binder. The presence of oxalic acid leads to the reaction with calcium carbonate, with the resulting formation of calcium oxalates [11, 15, 16]. Green pigments were also identified as green earths, such as in the hand of an angel surrounding the *mandorla* in the large rib vault (LR-22), consisting of green and pink tones that revealed the presence of green earth and hematite, combined with calcite and gypsum. Though, the low intensity of the signal related to the green pigment did not allow to distinguish between celadonite and glauconite [10].

The presence of organic binders as lipids and proteinaceous materials was assessed by GC–MS investigations on six samples (SF1, SF2, SF3, SF4, SF5 and SF6) (Table 4).

We have seen the peak of azelaic (nonanedioic acid, saturated dicarboxylic acid), miristic (C14:0), palmitic (C16:0), oleic (C18:1) and stearic (C18:0) acids. In particular, we have considered the ratio azelaic acid/palmitic acid, which, being lower than one, allows to exclude the presence of any specific siccativ oil [17]. A first very interesting result is that the lipid fraction detected is not attributable to a specific drying oil, allowing to say that the painting was not made using the traditional oil technique. It can be assumed that there is a mixture of oils consisting of a drying oil together with one or more non-drying or semi-drying oils. In the chromatograms relative to the amino acids fractions, the detection of alanine, glycine, threonine, serine, valine, leucine, proline, aspartic acid, glutamic acid and phenylalanine recommend the presence of proteinaceous binder. Figure 8 shows the chromatographic profile of SF3 sample.

Fig. 4 Raman spectra on red details: the mantle of Pope (LR-29), showing vermilion (v) and hematite (h) signals; the lateral decoration of the rib vault (LR-15), showing hematite signals. Traces of calcite are pointed out by the asterisk *

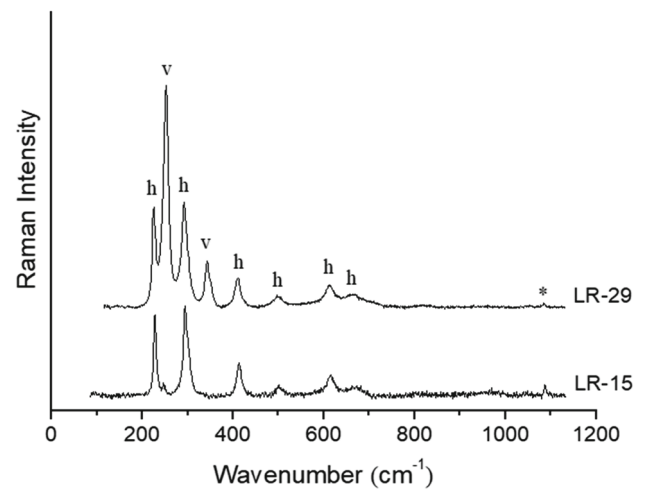


Fig. 5 Raman spectra on yellow details: a *pelta* frame of the large rib vault (LR-23), showing goethite signals; a decoration of racemes of flowers (LR-32), showing litharge signals. Traces of calcite and gypsum are pointed out by the symbol * and §, respectively

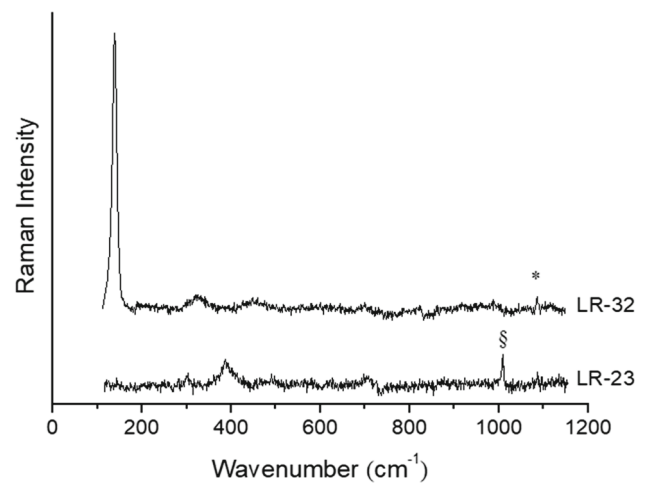
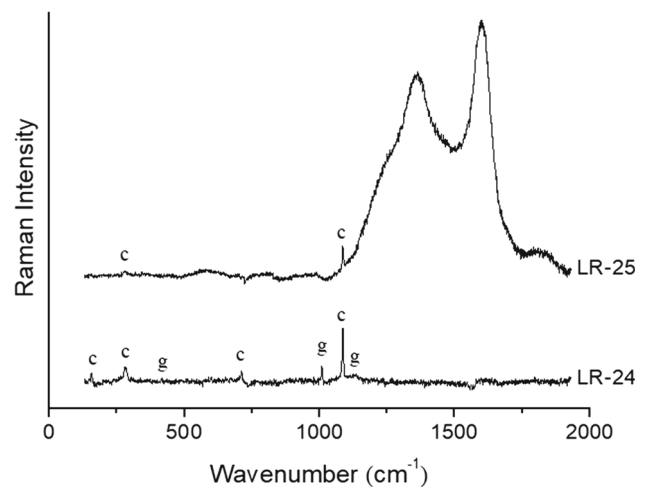


Fig. 6 Raman spectra on grey samples, showing calcite and gypsum signals in white details (LR-24) and amorphous carbon signals with traces of calcite in black details (LR-25)



To recognize the binding media, the percentage content of amino acids in each sample was compared to those from a dataset of 43 reference samples of egg (whole, egg white, egg yolk), casein, animal glue and mixture of them, going to the reference collection of the Opificio delle Pietre Dure in Florence, Italy [18]. Principal component analysis (PCA) was carried out on the correlation matrix of the relative percentage contents of eight amino acids (aspartic acid, glutamic acid, proline, hydroxyproline, phenylalanine, alanine, glycine and leucine) [19, 20]. The PCA score plot is reported in Fig. 9.

The samples collected are placed on the Cartesian diagram of the PCA not far from the Egg references, suggesting egg as a binder in all the samples.

Fig. 7 Raman spectra on blue and green samples: a green veining (LR-31), showing malachite signals; blue racemes in a clypeus (LR-33), showing azurite signals and in one case the characteristic signal of barite (b). In addition, weddellite signals were observed. Traces of calcite are pointed out by the asterisk *

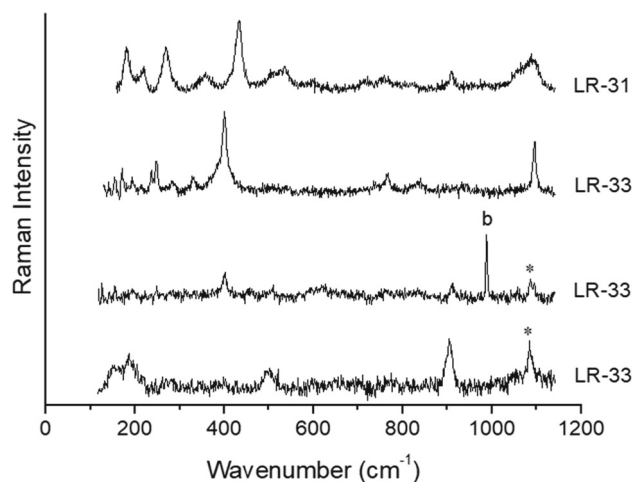
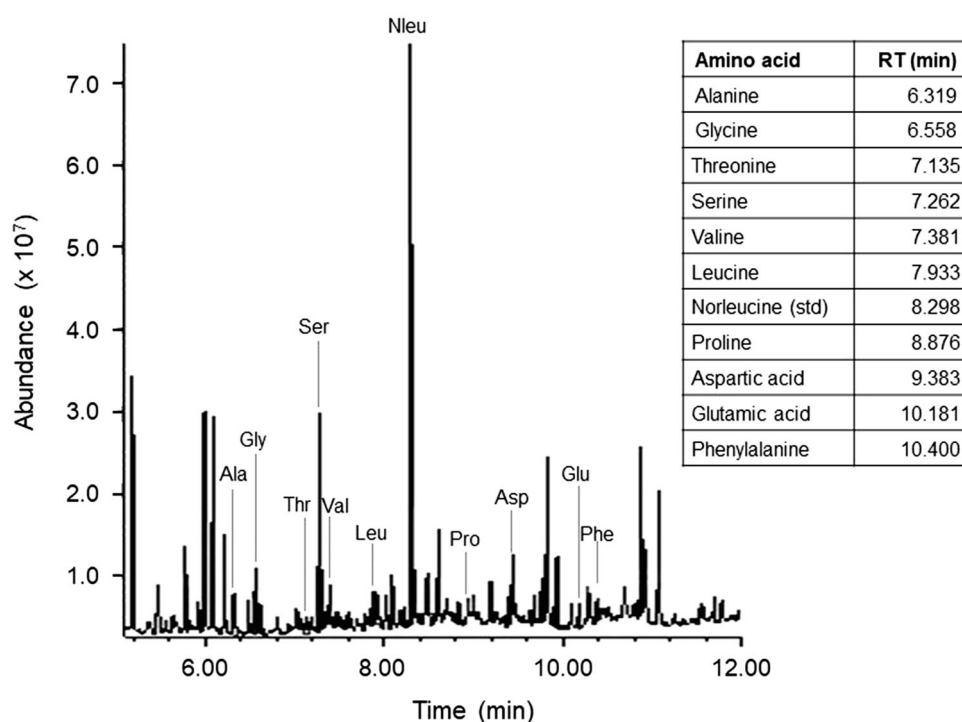


Table 4 Description of samples analysed by GC-MS

Sample	Colour	Analysed detail
SF1	Golden	Star in the sky (rib vault #3)
SF2	Blue	Sky (rib vault #4)
SF3	Green	Flower veining (vault)
SF4	Red	Flowers (wall #6)
SF5	Green	Leaves (wall #7)
SF6	Golden?	Jesus's mantle (keystone)

Fig. 8 GC-MS chromatogram of the proteinaceous fraction of SF3 sample. Ala = alanine, Gly = glycine, Thr = threonine, Ser = serine, Val = valine, Leu = leucine, Nleu = norleucine (internal standard), Pro = proline, Asp = aspartic acid, Glu = glutamic acid, Phe = phenylalanine. In the inset the retention times for each amino acid are reported



4 Conclusion

The in situ campaign performed on the 15th-century paintings in the church apse of S. Francesco del Prato in Parma (Italy) revealed essential information about the pigments used by the artists who realized the wall paintings. Through the mobile instruments, a quick and effective recognition of the main pigments was successfully achieved. Mobile Raman analyses identified a number of pigments (hematite, vermilion, lead tin yellow II, calcite and carbon black), whose chemical composition was typically supported

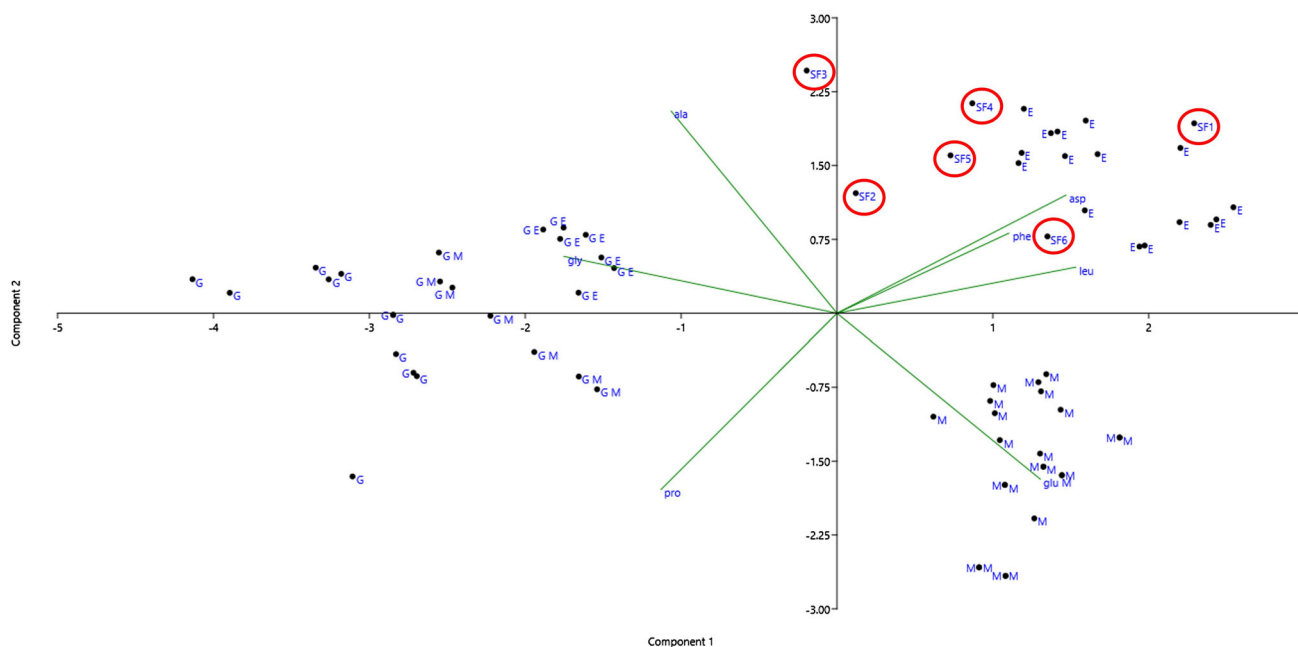


Fig. 9 PCA score plot of the relative percentage contents of eight amino acids in 43 paint samples from the collection of reference paint layers, stored at Opificio delle Pietre Dure in Florence, Italy, and artistic samples SF1, SF2, SF3, SF4, SF5 and SF6. The first two principal components, PC1 and PC2, account for 54,39% and 25,41% of the total variance, respectively. (G: animal glue; M: milk; E: egg; GE: animal glue and egg; GM: animal glue and milk; EM: egg and milk)

by the XRF analyses. Furthermore, the use of Cu-based pigments was suggested by XRF results. Laboratory analyses corroborated the understanding of the techniques, through the analysis of pigments and binders. In addition to the results obtained from the in situ measurements, which were confirmed by micro-Raman investigations, the identification of the colour palette was thoroughly revealed (goethite, litharge, green earths and barite), including also the use of *a secco* pigments (azurite and malachite) in some areas. Moreover, micro-Raman analyses detected degradation products due to the alteration of some pigments (gypsum and weddellite). Despite their low amounts compared to the original pigments, these compounds were effectively identified, thanks to the micro-scale investigation. GC–MS revealed protein- and lipid-based binders, mainly made by a compresence of siccative and semi-siccative oils and by egg.

Interestingly, the recent rediscovery of these valuable wall paintings was enriched by the results of the in situ Raman and XRF campaign and the laboratory micro-Raman and GC–MS investigations. In this study we obtained new information on pigments and binders were obtained on the 15th-century wall paintings, whose preciousness is highlighted by a rich colour palette and a focused use of different pigments according to the painted contents. These results are expected to be useful in the future studies that will deepen the recent recovery of the church of San Francesco del Prato.

Supplementary Information The online version contains supplementary material available at <https://doi.org/10.1140/epjp/s13360-023-03702-1>.

Acknowledgements The authors thank Prof Sergio De Iasio (Department of Chemical Science, Life and Environmental Sustainability, University of Parma) for his help in processing the chromatographic results.

Funding Open access funding provided by Università degli Studi di Parma within the CRUI-CARE Agreement.

Data Availability Statement The datasets generated and analysed during the current study are available from the corresponding author on reasonable request.

Open Access This article is licensed under a Creative Commons Attribution 4.0 International License, which permits use, sharing, adaptation, distribution and reproduction in any medium or format, as long as you give appropriate credit to the original author(s) and the source, provide a link to the Creative Commons licence, and indicate if changes were made. The images or other third party material in this article are included in the article's Creative Commons licence, unless indicated otherwise in a credit line to the material. If material is not included in the article's Creative Commons licence and your intended use is not permitted by statutory regulation or exceeds the permitted use, you will need to obtain permission directly from the copyright holder. To view a copy of this licence, visit <http://creativecommons.org/licenses/by/4.0/>.

References

1. N. Pelicelli, San Francesco Del Prato e i Frati Minori Di Parma Nel Secolo XIII (1926)
2. G. Zanotti, Aurea Parma **II**, (1975).
3. G. Zanichelli, Stor. Della Città Riv. Internazionale Di Stor. Urbana e Territ. **26/27**, 131 (1983).
4. A. F. Fiore and P. Marchetti, San Francesco Del Prato in Parma: Una Cattedrale Gotica Incarcerata (Tipografia Benedettina Editrice, 1998)
5. A. Casoli, S. Santoro, Chem. Cent. J. **6**, 1 (2012). <https://doi.org/10.1186/1752-153X-6-107>
6. I. Bonaduce, E. Ribechini, F. Modugno, M.P. Colombini, Top. Curr. Chem. **374**, 1 (2016). <https://doi.org/10.1007/s41061-015-0007-x>
7. D.L.A. De Faria, S. Venâncio Silva, M.T. De Oliveira, J. Raman Spectrosc. **28**, 873 (1997). [https://doi.org/10.1002/\(sici\)1097-4555\(199711\)28:11%3c873::aid-jrs177%3e3.0.co;2-b](https://doi.org/10.1002/(sici)1097-4555(199711)28:11%3c873::aid-jrs177%3e3.0.co;2-b)
8. L. Burgio, R.J.H. Clark, Spectrochim. Acta Part A Mol. Biomol. Spectrosc. **57**, 1491 (2001). [https://doi.org/10.1016/S1386-1425\(00\)00495-9](https://doi.org/10.1016/S1386-1425(00)00495-9)
9. D. Bersani, P.P. Lottici, J. Raman Spectrosc. **47**, 499 (2016). <https://doi.org/10.1002/jrs.4914>
10. F. Ospitali, D. Bersani, G. Di Lonardo, P.P. Lottici, J. Raman Spectrosc. **39**, 1066 (2008). <https://doi.org/10.1002/jrs.1983>
11. K. Castro, A. Sarmiento, I. Martínez-Arkarazo, J.M. Madariaga, L.A. Fernández, Anal. Chem. **80**, 4103 (2008). <https://doi.org/10.1021/ac800255w>
12. I. Costantini, P.P. Lottici, K. Castro, J.M. Madariaga, Minerals **10**, 1 (2020). <https://doi.org/10.3390/min10050468>
13. R.J.H. Clark, Comptes Rendus Chim. **5**, 7 (2002). [https://doi.org/10.1016/s1631-0748\(02\)01341-3](https://doi.org/10.1016/s1631-0748(02)01341-3)
14. D. Bersani, G. Antonioli, P.P. Lottici, A. Casoli, Spectrochim. Acta Part A Mol. Biomol. Spectrosc. **59**, 2409 (2003). [https://doi.org/10.1016/S1386-1425\(03\)00081-7](https://doi.org/10.1016/S1386-1425(03)00081-7)
15. A. Nevin, J.L. Melia, I. Osticioli, G. Gautier, M.P. Colombini, J. Cult. Herit. **9**, 154 (2008). <https://doi.org/10.1016/j.culher.2007.10.002>
16. M. Pérez-Alonso, K. Castro, J.M. Madariaga, Anal. Chim. Acta **571**, 121 (2006). <https://doi.org/10.1016/j.aca.2006.04.049>
17. J. Blaško, R. Kubinec, B. Husová, P. Příkryl, V. Pacáková, K. Štulík, J. Hradilová, J. Sep. Sci. **31**, 1067 (2008). <https://doi.org/10.1002/jssc.200700449>
18. G. Lanterna, A. Mairani, M. Matteini, M. Rizzi, and A. Vigato, in Proc. 2nd Int. Congr. Sci. Technol. Safeguard Cult. Herit. Mediterr. Basin 5--9 July 1999 (Elsevier, Paris, France, 1999), pp. 487–489
19. A. Casoli, L. Alberici, D. Cauzzi, and G. Palla, in Proc. 2nd Int. Congr. Sci. Technol. Safeguard Cult. Herit. Mediterr. Basin 5--9 July 1999 (Elsevier, Amsterdam, Netherlands, 2000), pp. 591–593
20. A. Casoli, A. Montanari, and G. Palla, in Proc. 3rd Int. Congr. Sci. Technol. Safeguard Cult. Herit. Mediterr. Basin 9--14 July 2001 (2001), pp. 839–845